

Soluble Imidazolium-Functionalized Coordination Cages for Efficient Homogeneous Catalysis of CO₂ Cycloaddition Reactions

Huiying Tong,^{a,c} Jun Liang,^b Qiujin Wu,^{a,c} Yuhuang Zou,^a Yuanbiao Huang,^{* a,c} and Rong Cao^{* a,c}

^aState Key Laboratory of Structural Chemistry, Fujian Institute of Research on the Structure of Matter, Chinese Academy of Sciences, Fujian, Fuzhou 350002, P. R. China;

^bHoffmann Institute of Advanced Materials, Shenzhen Polytechnic, 7098 Liuxian Blvd, Nanshan District, Shenzhen, 518055 China;

^cUniversity of Chinese Academy of Sciences, Beijing 100049, P. R. China

Email: ybhuang@fjirsm.ac.cn (Y.-B. Huang), rcao@fjirsm.ac.cn (R. Cao)

Experimental section:

1.1 Materials and instruments

2-(Imidazol-1-yl)terephthalic acid was synthesized according to previous report.¹ *p*-tert-Butylthiacalix [4] arene (H₄BTC4A)², *p*-tert-butylsulfonylcalix[4]arene (H₄BTC4A-SO₂)³ and ionic ligand (I)Im-H₂BDC⁴ were synthesized also as the previously reported method. Other reagents were obtained from commercials and used without further purification.

CO₂ sorption isotherms for compounds were measured by using a Micrometrics ASAP 2020 instrument at 273 K. Before the measurement, the samples were activated at 373 K in vacuum for 10 hours. Powder X-ray diffraction patterns (PXRD) were recorded on a Rigaku Dmax 2500 diffractometer equipped with Cu-K α radiation ($\lambda = 1.54056 \text{ \AA}$) over the 2θ range of 5-50° with a scan speed of 5° min⁻¹ at room temperature. Thermogravimetric analyses (TGA) were performed under a nitrogen atmosphere with a heating rate of 10 °C min⁻¹ by using an SDT Q600 thermogravimetric analyser. Infrared (IR) spectra were recorded using KBr pellets on a PerkinElmer Spectrum One in the range of 400-4000 cm⁻¹. Elemental analyses of C, H, and N were carried out on an Elementar Vario EL III analyzer. The ¹H NMR was performed at AVANCE III Bruker Biospin spectrometer, operating at 400 MHz. The ultraviolet-visible (UV-vis) spectra were collected at room temperature on a

Shimadzu UV-2550 spectrophotometer. The gas chromatography (GC) measurements were performed on a G7890A-GC equipped with a HP-5 column, FID detector and autosampler. EDS analyses recording were performed on a HITACHI S-4800 Field Emission Scanning Electron Microscope. Mass spectra were achieved with Bruker microTOF-Q II mass spectrometer in the electrospray ionization (ESI) mode.

X-ray Crystallography. Single crystal X-ray diffraction data for ImBDC-Co, ImBDC-Ni were collected on Rigaku XtaLAB Synergy-Coustom diffractometer equipped with Ga-K α radiation ($\lambda = 1.3405 \text{ \AA}$) at 100 K. We have collected several datasets for ImBDC-M (M = Co or Ni) using Ga-K α radiation. Among the several datesets for ImBDC-M (M = Co or Ni), the best dataset was used for structure solution and refinement. The structure of ImBDC-M (M = Co or Ni) was refined employing full-matrix least squares on F^2 using the latest version of the SHELX-2014 program.⁵ Hydrogen atoms were generated in their idealized positions and all nonhydrogen atoms were refined anisotropically. The disorder solvent in the void space of these crystals was calculated using the program SQUEEZE in PLATON software package. Because of the disordering of the solvent molecules and/or *t*-butyl groups in the structures, a number of restraints, such as FLAT, DFIX, SIMU and SADI, were applied to control the refinement. Besides, the imidazolium cations of the ligand were also disorder thus we used the PART -1/PART -2/PART -3/PART -4 to restraint it. However, due to the existence of flexible *t*-butyl groups and the imidazolium groups in the struture, the disordered vibration of these two crystals is very large, which makes it impossible to collect the diffraction points at high angles even at low temperature. CCDC 2041557 (ImBDC-Co) and 2041558 (ImBDC-Ni) contains the supplementary crystallographic data for this paper.

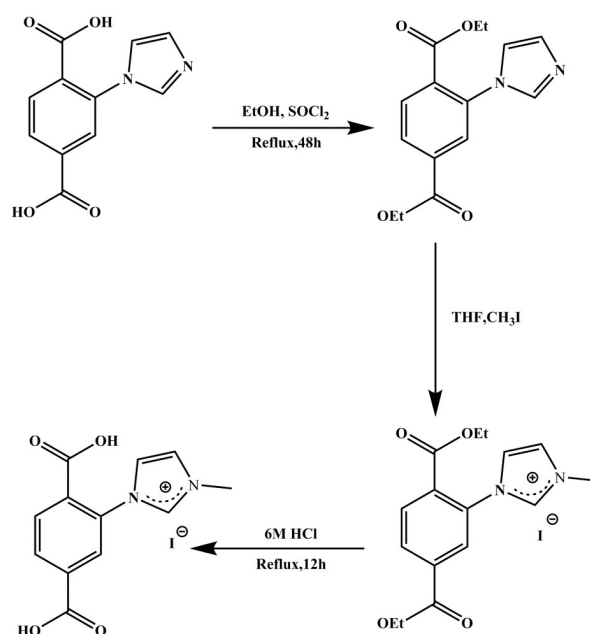
1.2 In suit FT-TR spectra measurements

In situ FT-IR spectra of cycloaddition reaction of ImBDC-Co catalyzed CO₂ with epoxide was qualitatively performed on the NICOLET 6700 instrument at 353K. Before the measurement, the catalyst was activated at 373 K in vacuum for 12 h. Firstly, about 30 mg of ImBDC-Co was added into the reaction tank and a CO₂ atmosphere of 0.1 MPa was introduced. After five minutes, pure Ar was used to dilute the CO₂ until a suitable and stable carbon dioxide signal strength was detected. Turn off Ar, drop 0.1 ml of styrene oxide on the surface of the catalyst, seal the reaction tank, and then heat it to 353K while monitoring the signal in real time.

Table S1. Crystal data and structure refinement for ImBDC-Co and ImBDC-Ni.

Identification code	ImBDC-Co	ImBDC-Ni
Empirical formula	C ₃₉₀ H ₃₅₄ Co ₂₄ I _{0.42} N ₂₄ O ₁₂₆ S ₂₄	C ₃₉₀ H _{343.33} I _{2.28} N ₂₄ Ni ₂₄ O ₁₂₆ S ₂₄
Formula weight	9630.01	9849.37
Temperature (K)	103(4) K	293(2)K
Crystal system	Tetragonal	Tetragonal
Space group	<i>I</i> 4/m	<i>I</i> 4/m
Unit cell dimensions	<i>a</i> = 29.4220(4) Å	<i>a</i> = 29.1997(5) Å
	<i>b</i> = 29.4220(4) Å	<i>b</i> = 29.1997(5) Å
	<i>c</i> = 40.2880 Å	<i>c</i> = 40.4454 Å
	$\alpha = 90^\circ$	$\alpha = 90^\circ$
	$\beta = 90^\circ$	$\beta = 90^\circ$
	$\gamma = 90^\circ$	$\gamma = 90^\circ$
Volume (Å ³)	34875.5(12)	34484.7(16)
Z	2	2
Density (calculated) (g·cm ³)	0.917	0.949
Absorption coefficient (mm ⁻¹)	3.815	4.833
F(000)	10297.0	10072
Crystal size (mm ³)	0.12 x 0.12 x 0.12	0.2 x 0.2 x 0.2
Reflections collected / unique	69449 / 13081 [R(int) = 0.0540]	69306/12857 [R(int) = 0.0753]
Data / restraints / parameters	13081 / 3571 / 1004	12857/3589/1015
Goodness-of-fit on <i>F</i> ²	1.154	1.325
Final <i>R</i> indices [I>2sigma(I)]	<i>R</i> ₁ = 0.0875 <i>wR</i> ₂ = 0.2801	<i>R</i> ₁ = 0.1121 <i>wR</i> ₂ = 0.3317
Final <i>R</i> indices (all data)	<i>R</i> ₁ = 0.1105 <i>wR</i> ₂ = 0.2982	<i>R</i> ₁ = 0.1524 <i>wR</i> ₂ = 0.3583

1.3 Synthesis of (I)Im-H₂BDC



Scheme S1. The synthesis of (I)Im-H₂BDC.

2-(imidazol-1-yl)terephthalic acid (12 mmol, 3.21 g) was dissolved in ethanol (40 mL) and added two drops DMF. Thionyl chloride (60 mmol, 4.4 mL) was added dropwise under stirring. The mixture was refluxed at 80 °C for 48 h before cooling down to room temperature. The pH was adjusted to above 9 with 2 mol/L KOH. Then, within ten minutes, the solution was extracted with EtOAc (45 mL) four times. After removing the solvent, a white solid as diethyl 2-(imidazol-1-yl)terephthalate was obtained.

Each diethyl 2-(imidazol-1-yl)terephthalate (1 mmol, 0.288 g) was dissolved in 4 mL THF and then added 0.3 mL methyl iodide. The mixture was stirred in the Teflon-lined autoclave for half an hour before being sealed and heated at 100 °C for 24 hours. After cooling down to room temperature, the solvent was removed and the residue was dried under vacuo overnight.

Then, the obtained solid was dissolved in 20 mL 6 M HCl and the mixture was refluxed for 12 hours. The solvent was removed and the residue was dried fully under vacuo to give (I)Im-H₂BDC.

¹H NMR (400 MHz, DMSO-d₆, 25 °C) δ (ppm) = 3.95 (3H, CH₃), 7.89 (1H, N-CH-CH-N), 8.06 (1H, N-CH-CH-N), 8.20-8.29 (3H, Ar-H), 9.53 (1H, N-CH-N), 13.86 (2H, COOH).

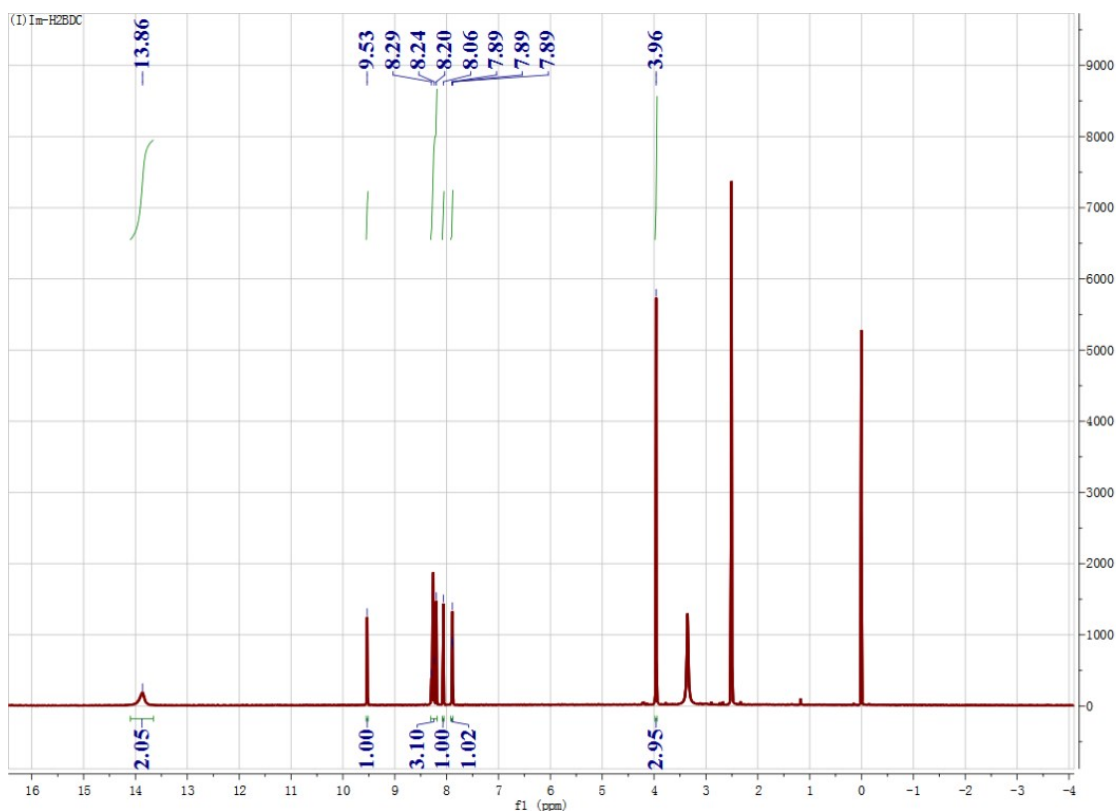


Fig. S1 ^1H NMR spectrum of (I)Im-H₂BDC in DMSO-d₆ (r.t.).

1.4 Synthesis of MOCs

Synthesis of ImBDC-Co.

A mixture of H₄BTC4A-SO₂ (0.01 mmol), CoCl₂·6H₂O (0.04 mmol) and (I)Im-H₂BDC (0.02 mmol) in N,N-dimethylacetamide/CH₃OH (1.5 / 2 mL) was sealed in a scintillation vial (10 ml capacity). Then the vial was transferred to a programmable oven and heated at a rate of 1.2°C/min from 30 °C to 100 °C. The temperature was held at 100 °C for 24 h before cooling to 30 °C at 100 °C for 2 day before cooling down to 30 °C at a rate of 0.05 °C/min. This procedure resulted in a clear dark blue solution, which was then placed in a stable environment at room temperature. After a week, purple crystals of ImBDC-Co was obtained, then washed by frozen DMA/CH₃OH (1.5 / 2 mL) three times.

Synthesis of ImBDC-Ni.

H₄BTC4A-SO₂ (0.01mmol), NiSO₄·6H₂O (0.04 mmol) and (I)Im-H₂BDC (0.02 mmol) in DMA/CH₃OH (1.5/2 mL) was sealed in a scintillation vial (10ml capacity). And the mixture was heat at 100 °C for 24 h. After cooling down to 30 °C a clear dark yellow solution was obtained, which was placed in a stable environment for one week. Then bright yellow crystals of ImBDC-Ni were obtained which washed by frozen DMA/CH₃OH (1.5 / 2 mL) three times.

Synthesis of MOSC-II -tBu-Co.⁶

H₄BTC4A-SO₂ (84.9 mg, 0.10 mmol), Co(NO₃)₂·6H₂O (145 mg, 0.5 mmol), and H₂BDC (54.8 mg, 0.33 mmol) were dissolved in 10 ml of N,N-dimethylformamide (DMF). The vial was then transferred to a programmable oven and heated at a rate of 0.5 °C/min from 35 to 100 °C. The temperature was held at 100 °C for 24 h before cooling to 35 °C at a rate of 0.2 °C/min.

Activation of MOCs for CO₂ absorption: the obtained samples were washed with frozen DMA/ CH₃OH (v/ v=1.5 / 2) for three times. Soaked in DMA/ CH₃OH (v/ v=1.5 / 2) for 20h and replaced the fresh solvent every 4h. Because of the cages have bigish DMA/ CH₃OH solubility, so the amount of DMA/ CH₃OH used was controlled (~5 mL per wash) to minimize loss of material. Repeated above operation with diethyl ether. Then dry in a vacuum oven at 100°C for 2 hours.

1.5 Catalytic performance evaluation

Cycloaddition of CO₂ with epoxides:

In a typical experiment, activated ImBDC-Co (29mg) of catalyst and 3 mmol epichlorohydrin were placed in a 15mL Schlenk tube fitted with a magnetic stirrer. After being sealed, the tube was purged thrice with CO₂. Then the reaction was conducted at 100 °C for 6 h under 1 atm carbon dioxide atmosphere. When using other epoxides, the reaction was carried out at 120 °C for 24 h under constant 1atm CO₂.

When the reaction finished, small amounts of the mixture was withdrew, diluted with ethanol and filtered with a 0.22 μm membrane filter. The qualitative analysis of product was determined by GC-MS and quantitative analysis by GC.

Recyclability experiment of ImBDC-Co:

The recyclability experiment was carried out as follows: after ethanol was added, the catalyst can be precipitated from the substrate and was separated by centrifugation, then washed by ethanol twice. After being dried at 70 °C for 12 hours in vacuum, the catalyst was used in the next catalytic reaction.

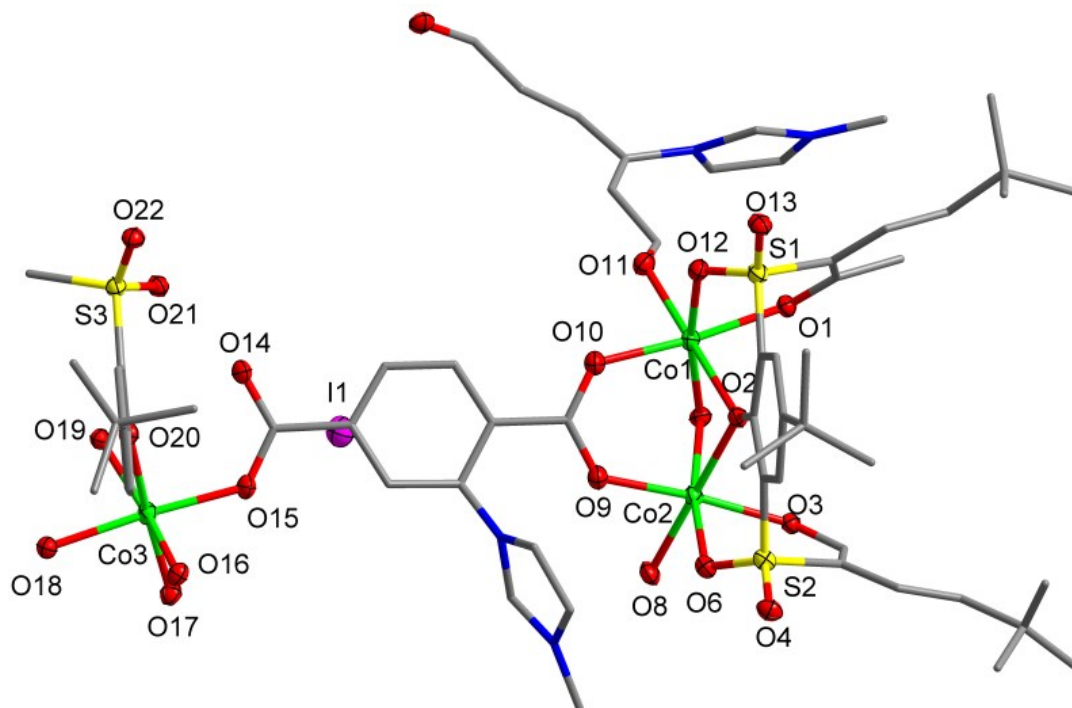


Fig. S2 The asymmetric unit in ImBDC-Co (H atoms are omitted).

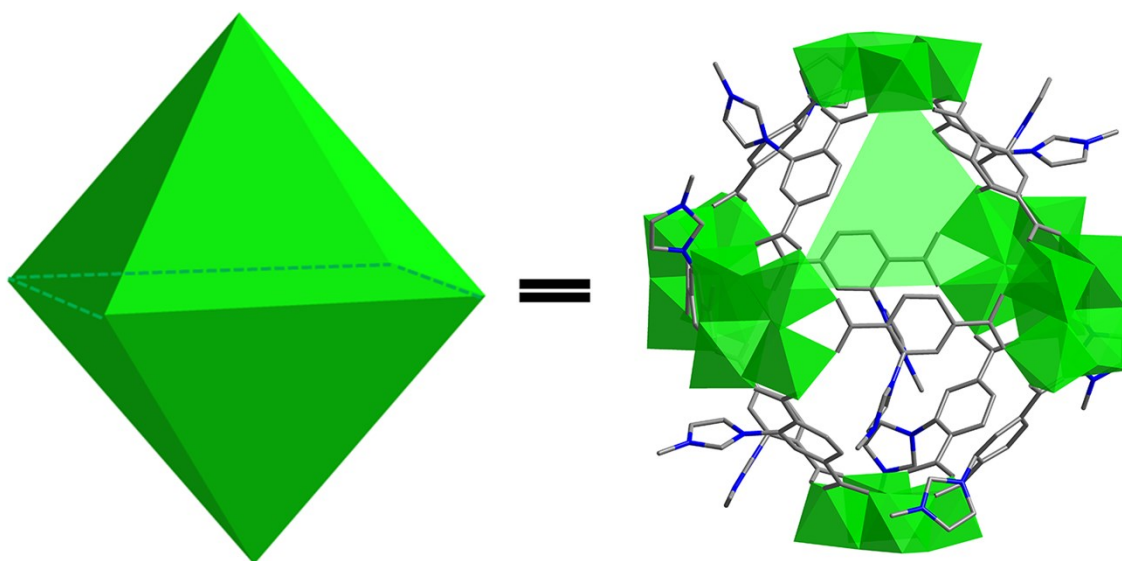


Fig. S3 Trigonal window of octahedral coordination cage. The *p*-tert-butylsulfonylcalix[4]arene ligands and H atoms are omitted for clarity.

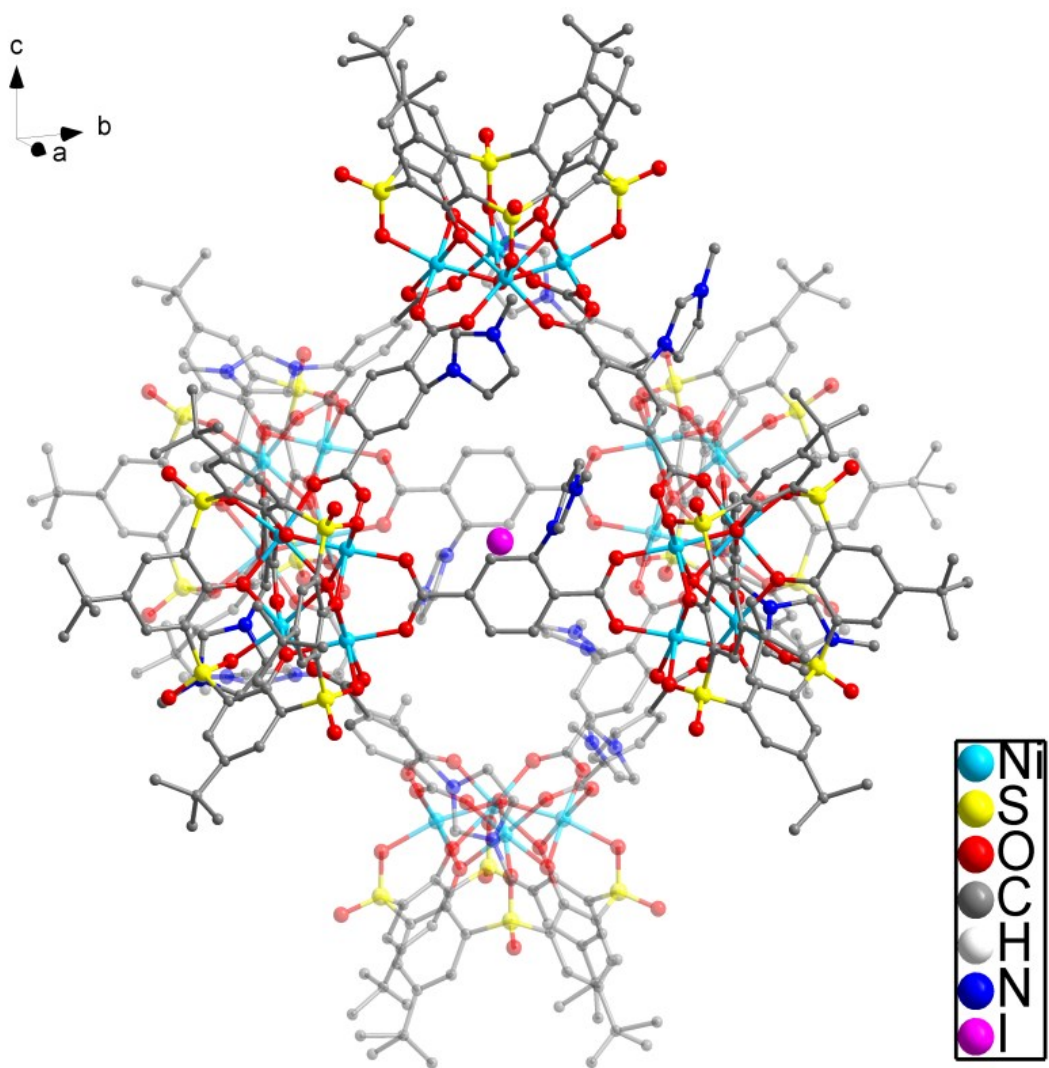
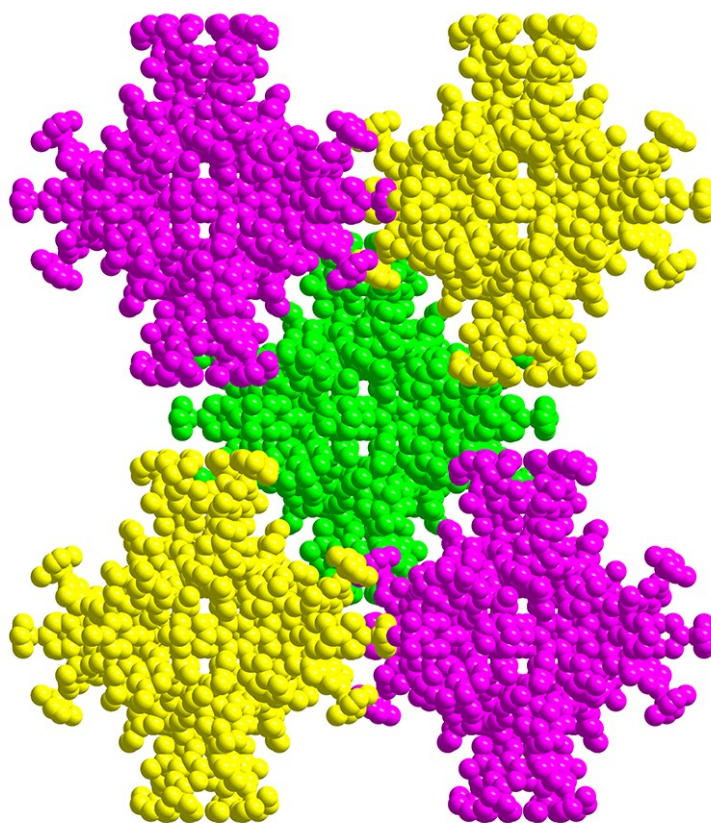


Fig. S4 Chemical structure of a cage in ImBDC-Ni. H atoms are omitted for clarity.

(a)



(b)

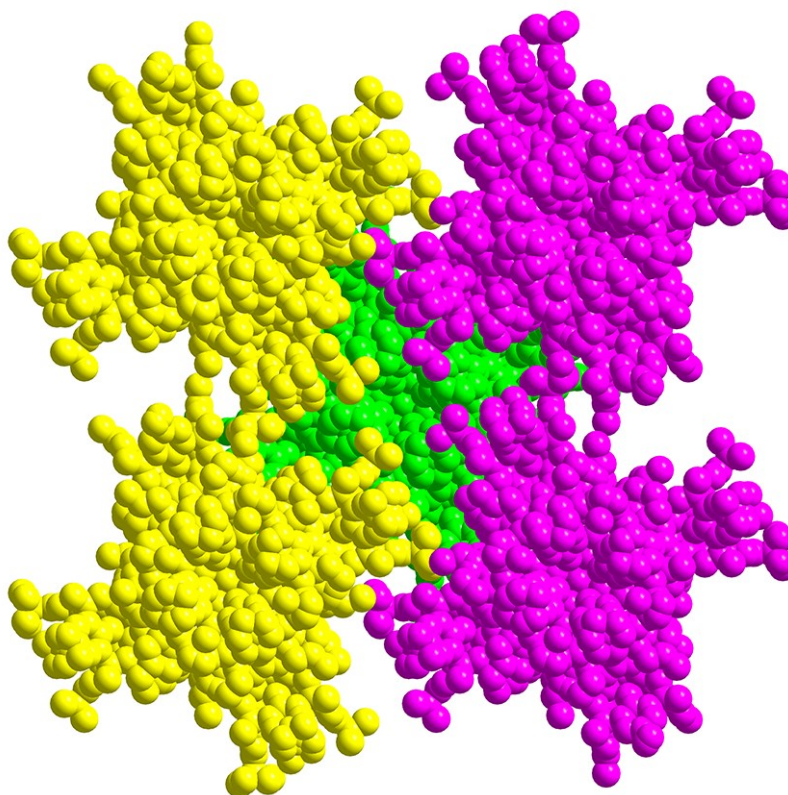


Fig. S5 (a) Pseudo body-centered cubic packing of ImBDC-Co view along the b axis and (b) c axis.

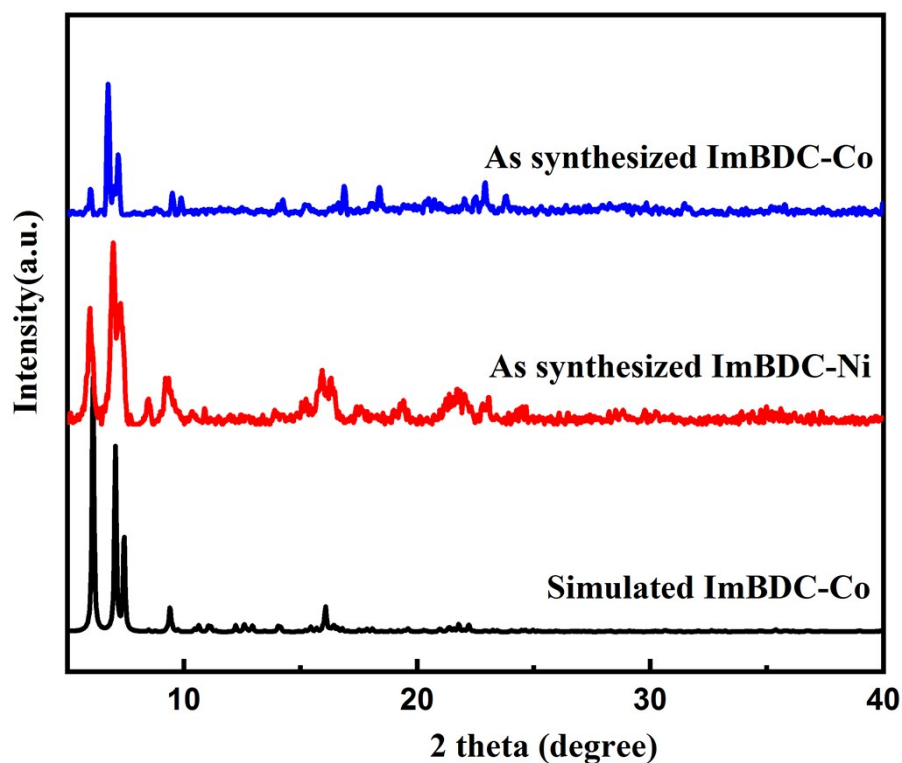


Fig. S6 PXRD patterns of ImBDC-Co and ImBDC-Ni.

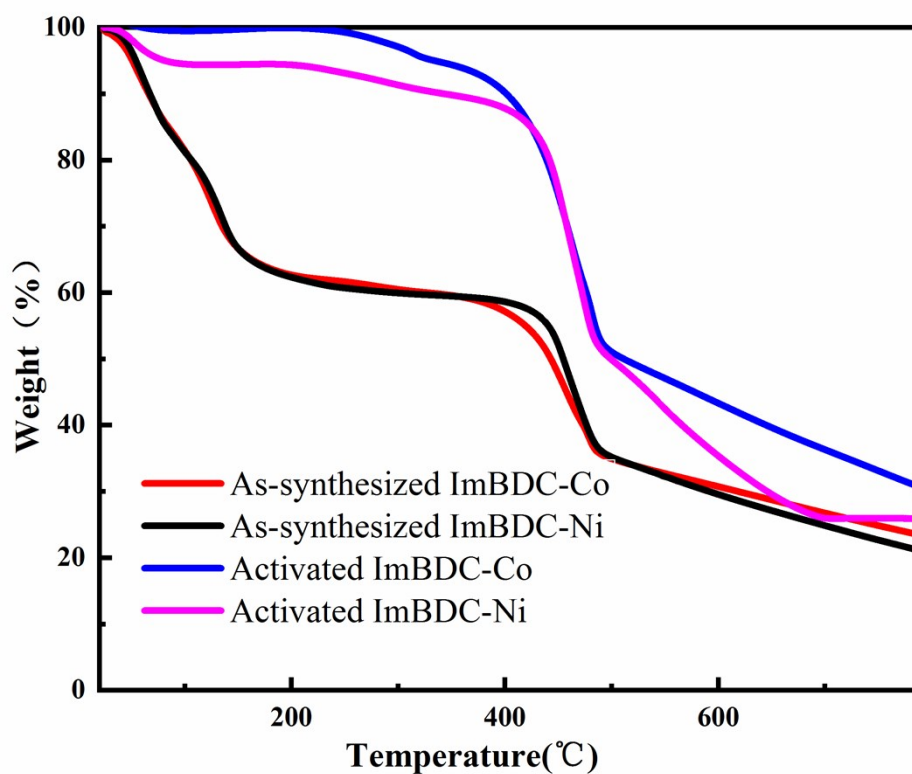


Fig. S7 TGA curves of as-synthesized and activated ImBDC-Co and ImBDC-Ni, respectively.

The ca. 35 wt% loss before 200 °C is attributed to the removal of guest molecules (DMA and H₂O) in ImBDC-Co and ImBDC-Ni.

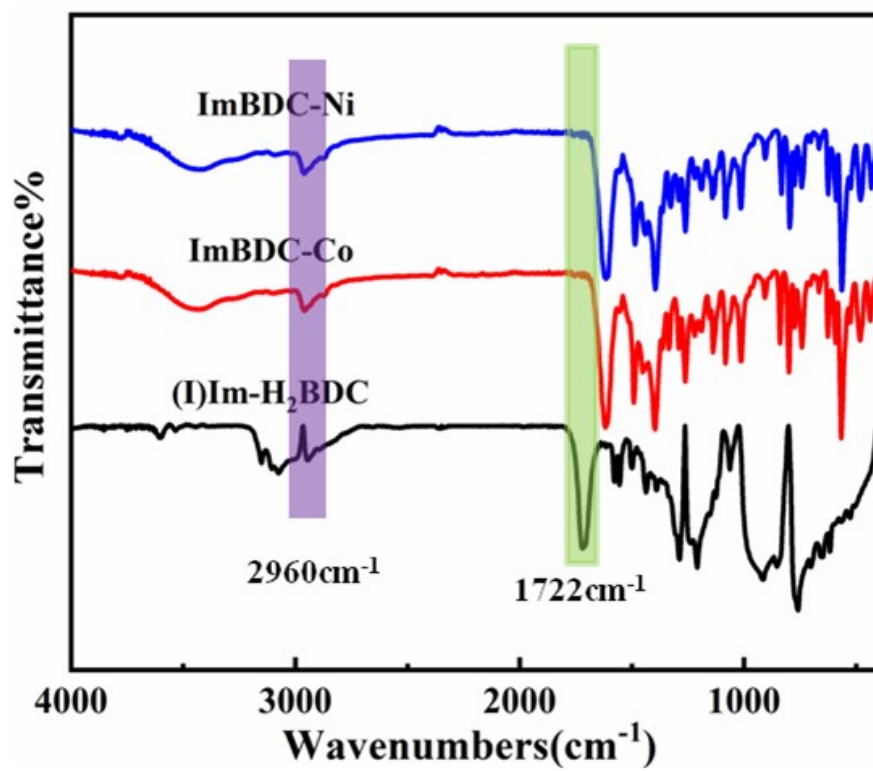


Fig. S8 FTIR spectra of ImBDC-Co and ImBDC-Ni.

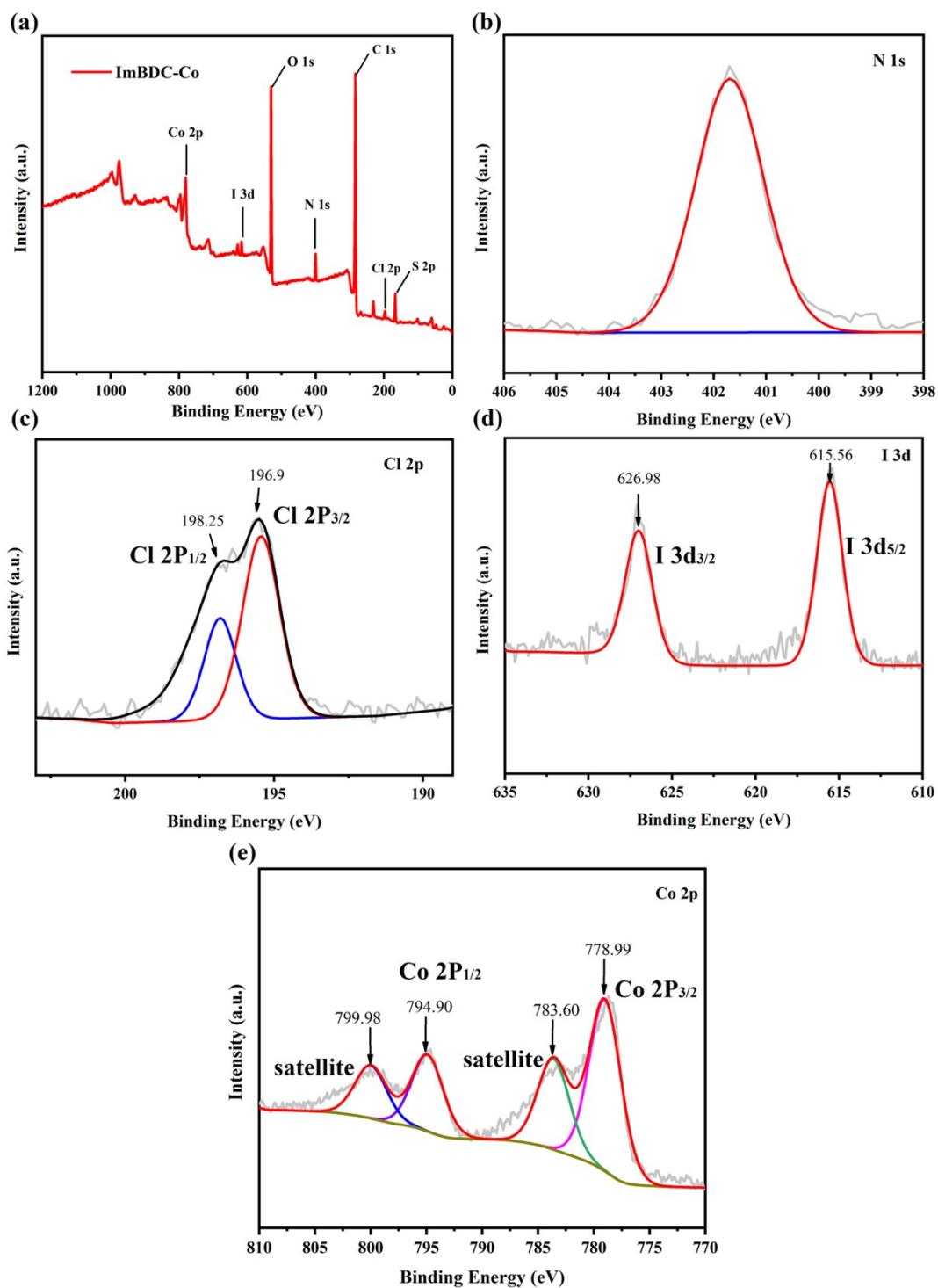


Fig. S9 XPS survey spectra (a) for ImBDC-Co, XPS spectra of N 1s (b), Cl 2p (c), I 3d(d) and Co 2p (e) in the ImBDCCo.

The peaks centered at 198.5 eV and 196.9 eV are attributed to Cl 2P_{1/2} and Cl 2P_{3/2}, confirming that ImBDC-Co contains free Cl⁻ anions (Fig. S9c.). The I 3d core-level spectrum of ImBDC-Co shows peaks at 615.6 eV and 627.0 eV, indicating the presence of free I⁻ (Fig. S9d).

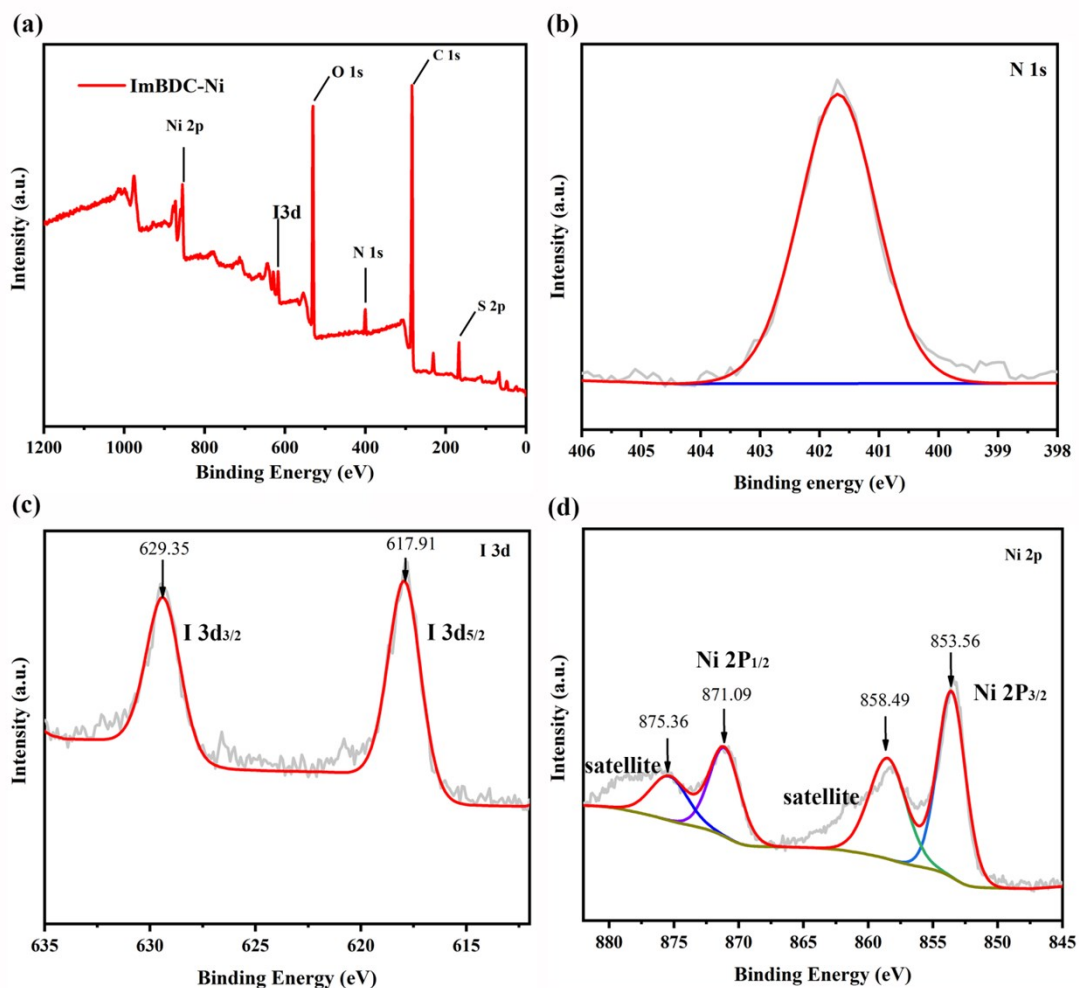


Fig. S10 XPS survey spectra (a) for ImBDC-Ni, XPS spectra of N 1s (b), I 3d (c), and Ni 2p (d) in the ImBDC-Ni.

The I 3d core-level spectrum of ImBDC-Co shows peaks at 617.9 eV and 629.3 eV, indicating the presence of free I⁻ (Fig. S10c).

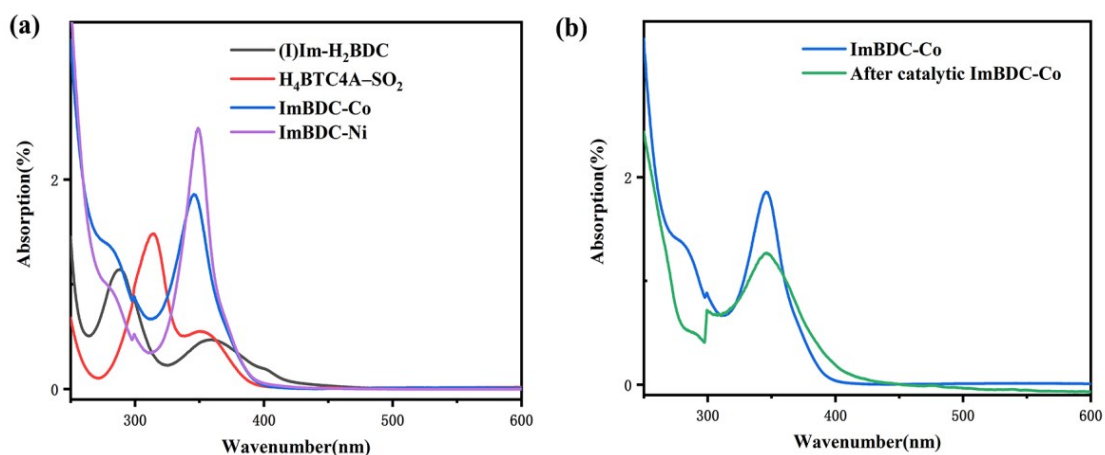


Fig. S11 UV-vis of (a) (I)Im-H₂BDC, H₄TBC4A-SO₂, ImBDC-Co and ImBDC-Ni, (b) fresh ImBDC-Co and ImBDC-Co after catalysis in CH₃OH at room temperature.

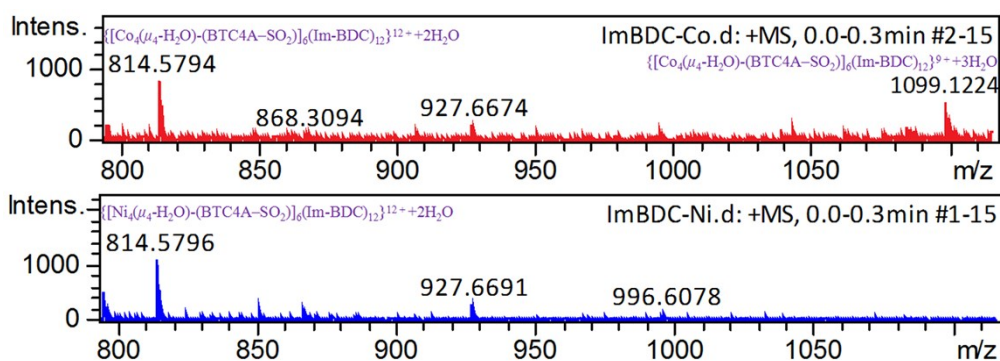


Fig. S12 MS spectra of ImBDC-Co(upper) and ImBDC-Ni (bottom).

UV-vis spectra (Figure S11a) and EIS-MS (Figure S12) demonstrated that the octahedral cages of ImBDC-Co and ImBDC-Ni remain intact in methanol. Thus, the good solubility of these MOCs in liquid epoxide enables them to be used as homogeneous catalysts for the CO₂ cycloaddition reaction.

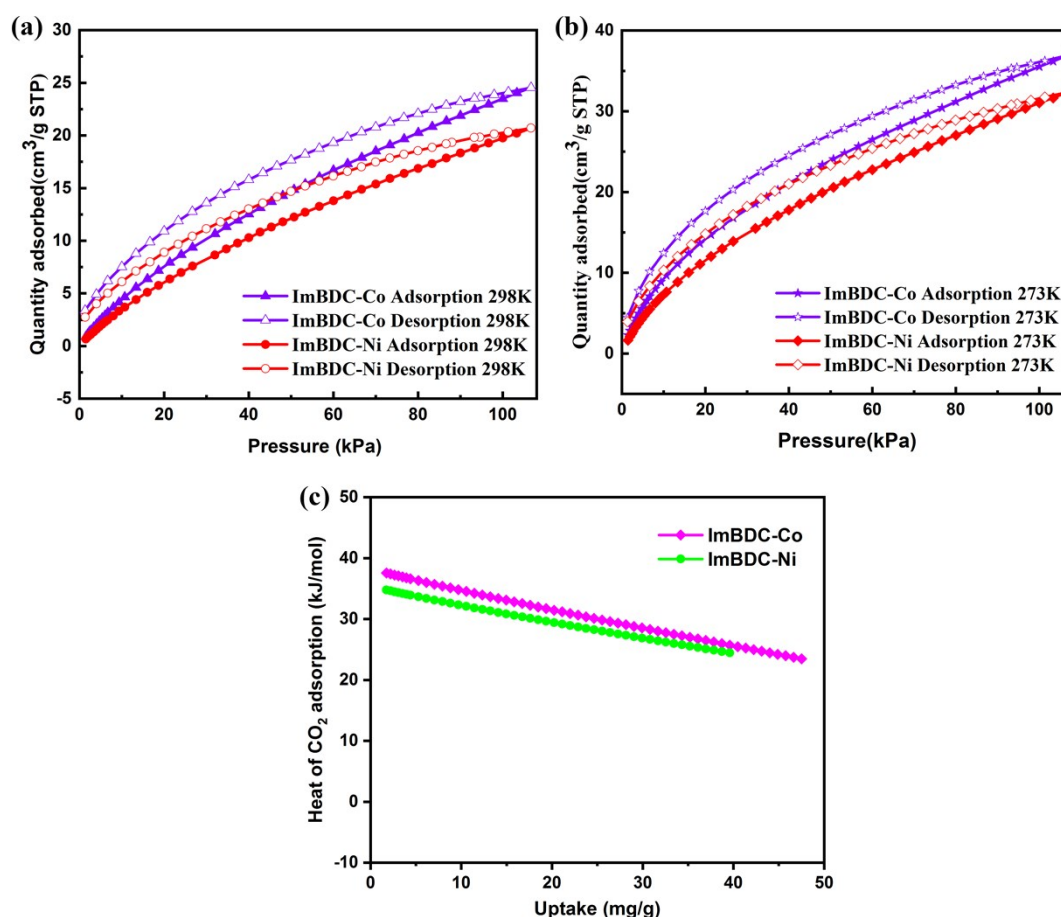


Fig. S13 (a) CO₂ absorption/desorption curves of ImBDC-Co and ImBDC-Ni at 298 K. (b) CO₂ sorption isotherms for ImBDC-Co and ImBDC-Ni at 273 K. (c) Isothermic enthalpy of adsorption CO₂ of ImBDC-Co and ImBDC-Ni at low coverage.

The isosteric enthalpy of adsorption CO_2 at zero loading (ΔH_{ads}^0) of ImBDC-Co and ImBDC-Ni were calculated based on the adsorption data collected at 298 and 273 K up to 1 bar (Fig. S14a and S14b). The $-\Delta H_{ads}^0$ values of ImBDC-Co and ImBDC-Ni were 37.6 and 34.8 kJ/mol (Fig. S14c), respectively. The high CO_2 adsorption uptakes and $-\Delta H_{ads}^0$ values for the two iMOCs highlights the key role of the imidazolium groups in the cages, which provide strong affinity for carbon dioxide via the dipole-quadruple interaction. Thus, their CO_2 -philic and large cavity features could facilitate in the enrichment of CO_2 near the imidazolium sites, which would be crucial for the catalytic conversion of CO_2 under mild conditions.

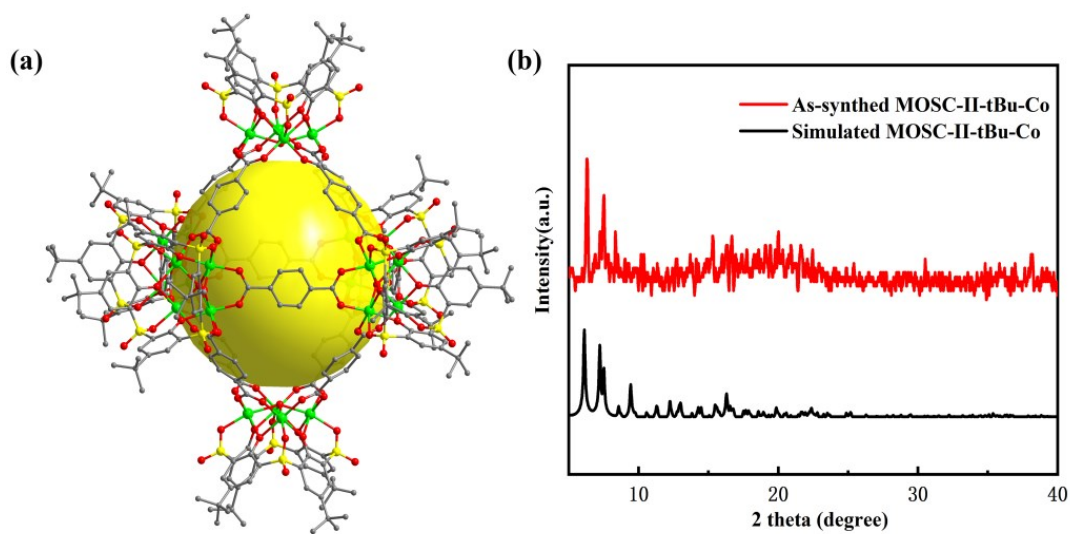


Fig. S14 (a) Crystal structure of MOSC-II-tBu-Co and (b) PXRD patterns of MOSC-II-tBu-Co.

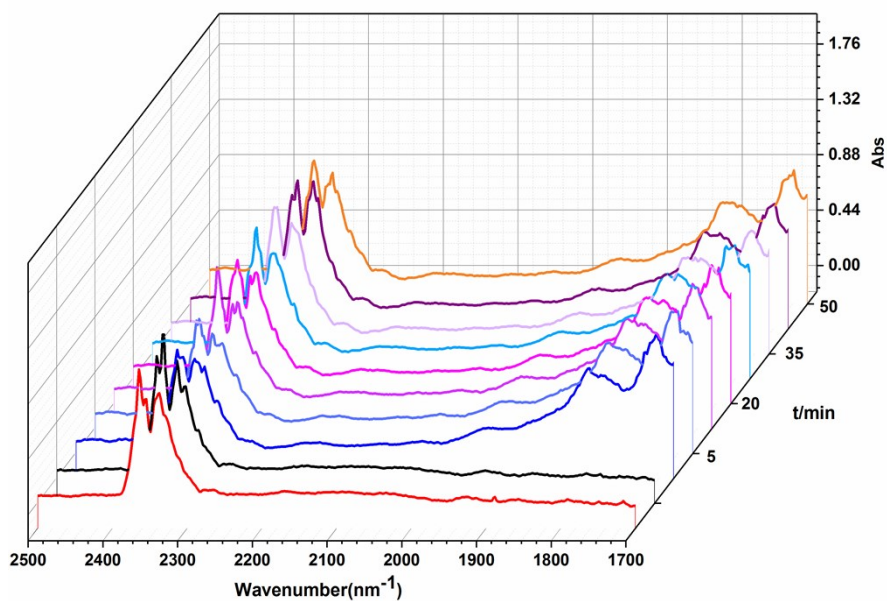


Fig. S15 *In situ* FT-IR spectra of produced chloroprene carbonate catalyzed by ImBDC-Co at 100 °C.

The newly appeared peaks of 1722 cm^{-1} and 1813 cm^{-1} belonged to the characteristic carbonyl peaks [$\nu(\text{C}=\text{O})$], and their intensities increased with reaction time, indicating the formation of chloropropylene carbonate. Moreover, the emergence and disappearance of a new peak at 2329 cm^{-1} during the reaction process was also observed as previously described in a heterogeneous system^{5a}, which might be attributed the attack of CO_2 molecules by anionic intermediate (Fig. S16, stage III). The result confirmed that the halogen anions play a key role for the CO_2 cycloaddition reaction with epoxides to form cyclic carbonates.

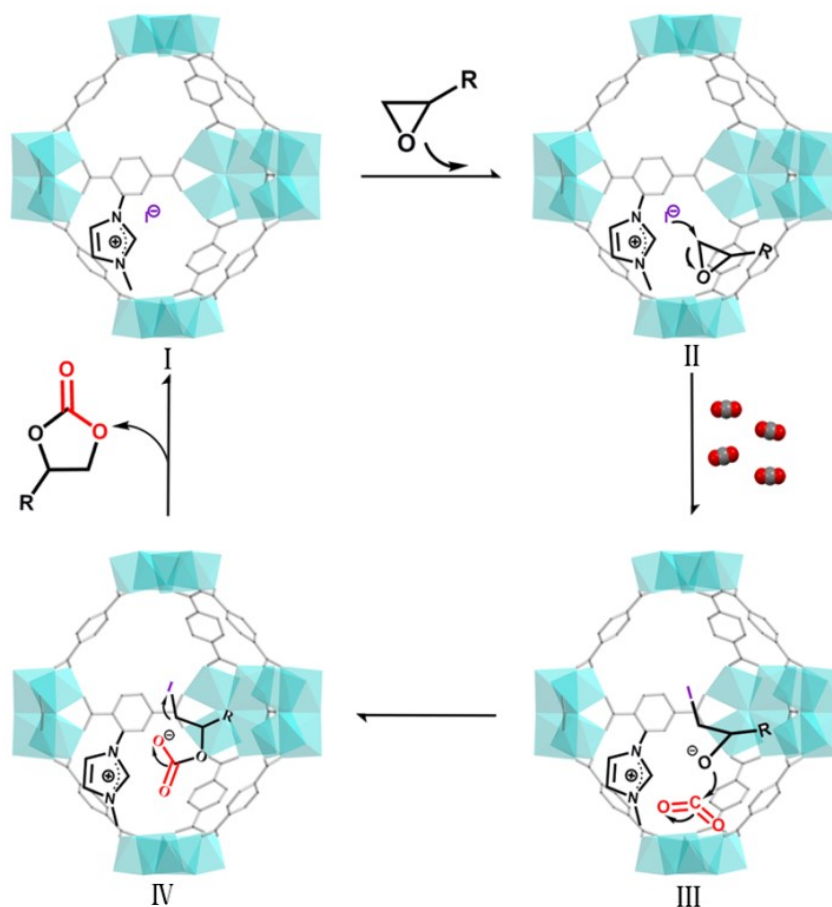


Fig. S16 Possible mechanism of catalytic cycloaddition reaction of CO_2 by ImBDC-Co. The *p*-tert-butylsulfonylcalix[4]arene anions and H atoms are omitted, and only one imidazolium group is shown for clarity.

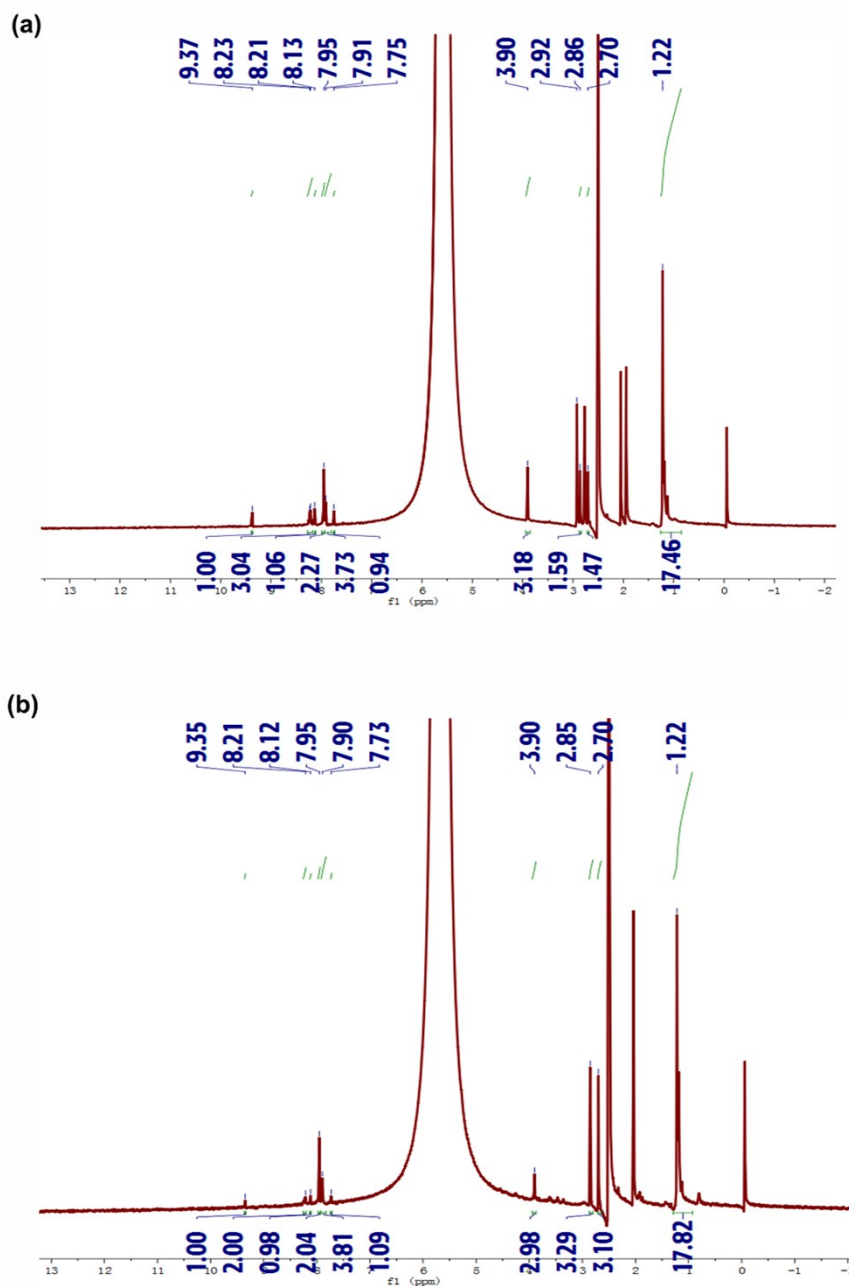


Fig. S17 ^1H NMR spectrum of (a) digested as synthesized ImBDC-Co and (b) digested ImBDC-Co sample after catalysis by the use of $\text{DMSO-}d_6$ (HF).

The ^1H NMR spectrum of digested ImBDC-Co (fresh and after catalysis) exhibited the same peaks of (I)Im- H_2BDC (3.90, CH_3 ; 7.75, N-CH-CH-N; 8.13, N-CH-CH-N; 8.21-8.23, Ar-H; 9.53, N-CH-N) and $\text{H}_4\text{BTC4A-SO}_2$ (7.91, Ar-H; 1.22, $\text{C}(\text{CH}_3)_3$). Therefore, the ratio of (I)Im- $\text{H}_2\text{BDC}/\text{H}_4\text{BTC4A-SO}_2$ (12:6) is obtained by integrating the peak areas.

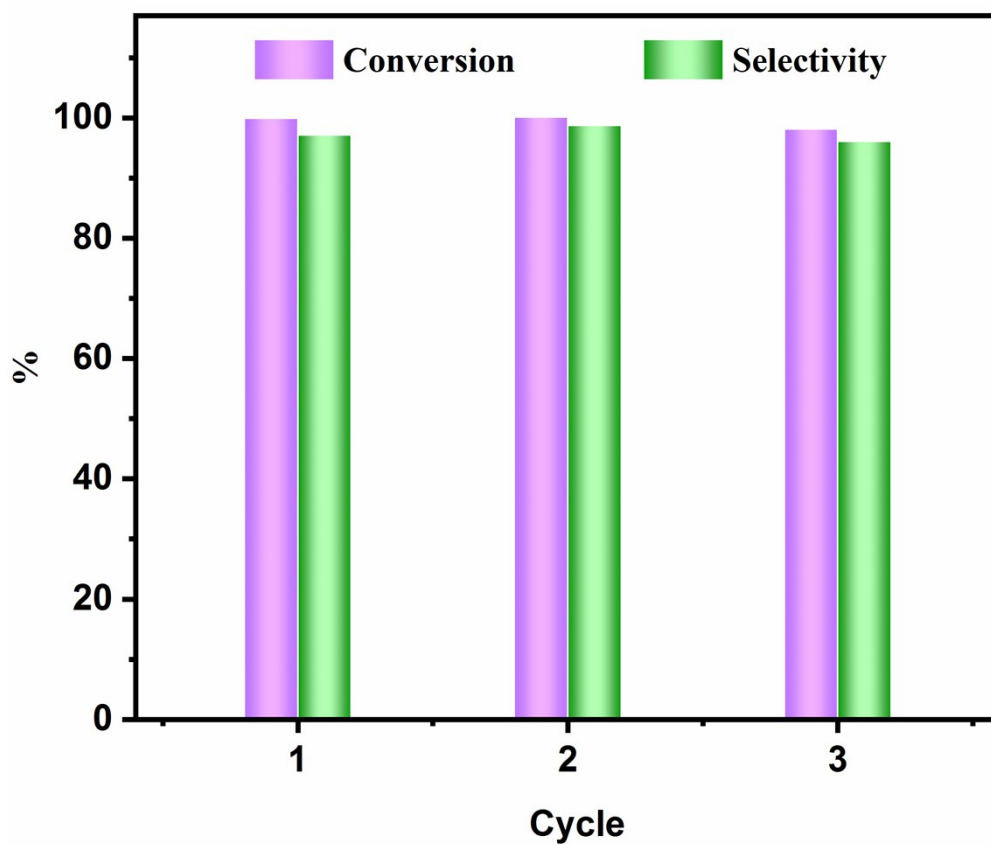


Fig. S18 Catalytic recycled experiment of ImBDC-Co. Reaction conditions: epichlorohydrin (3.0 mmol), ImBDC-Co (29 mg), temperature (100 °C), time (24 h), CO₂ (constant 1 atm).

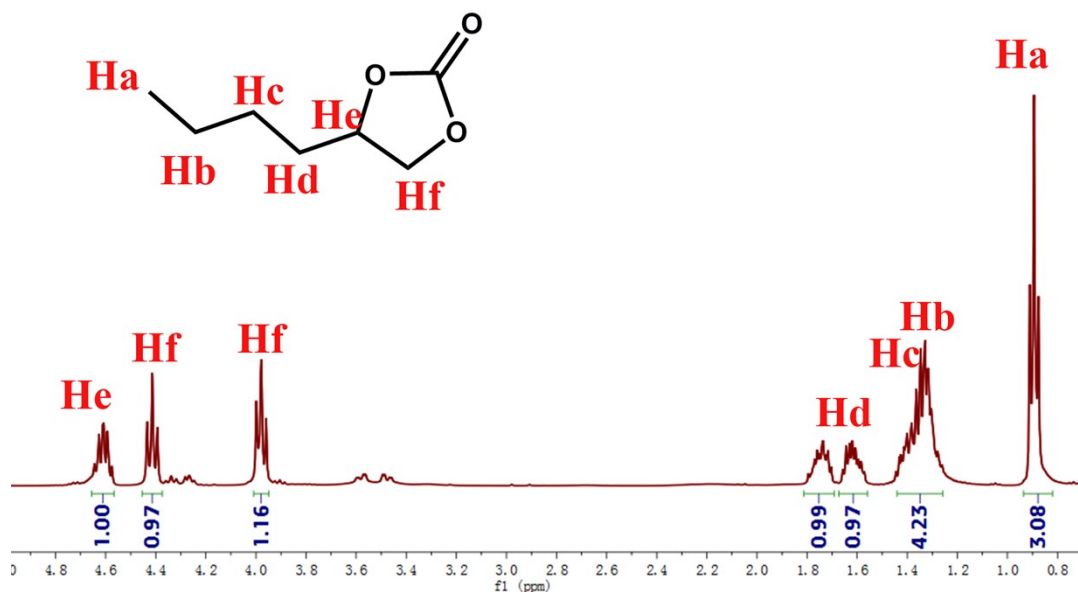


Fig. S19 ^1H NMR of the catalytic product through cycloaddition of CO_2 and 1,2-epoxybutane (CDCl_3). $\delta = 0.90\text{-}0.95$ (t, 3H), $1.35\text{-}1.47$ (m, 4H), $1.68\text{-}1.74$ (m, 1H), $1.77\text{-}1.82$ (m, 1H), $4.07\text{-}4.10$ (t, 1H), $4.54\text{-}4.57$ (t, 1H), $4.71\text{-}4.76$ (m, 1H).

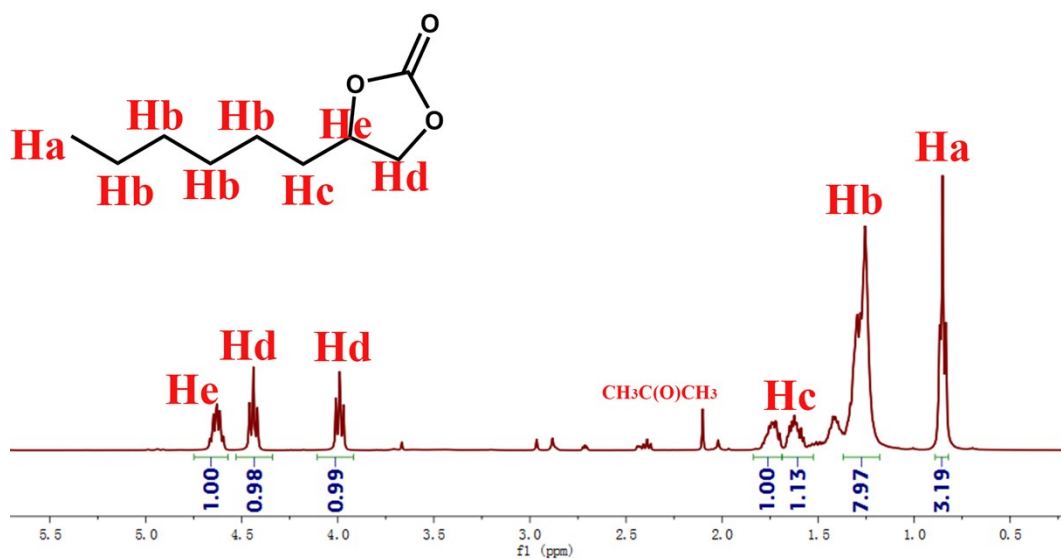


Fig. S20 ^1H NMR of the catalytic product through cycloaddition of CO_2 and 1,2-epoxyoctane (CDCl_3). $\delta = 0.83\text{-}0.87$ (t, 3H), $1.26\text{-}1.30$ (m, 8H), $1.62\text{-}1.66$ (m, 1H), $1.70\text{-}1.75$ (m, 1H), $3.97\text{-}4.01$ (t, 1H), $4.42\text{-}4.46$ (t, 1H), $4.60\text{-}4.67$ (m, 1H).

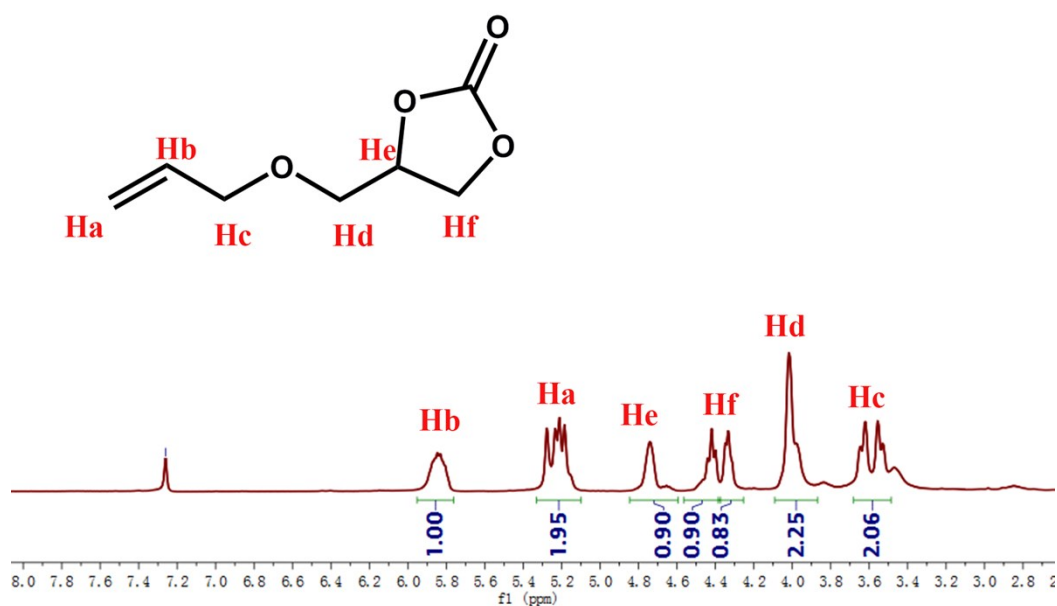


Fig. S21 ^1H NMR of the catalytic product through cycloaddition of CO_2 and 1-allyloxy-2,3-epoxypropane (CDCl_3). $\delta = 3.53\text{--}3.64$ (m, 2H), 3.98-4.02 (m, 2H), 4.36 (dd, 1H), 4.49 (t, 1H), 4.74 (m, 1H), 5.18-5.28 (m, 2H), 5.85 (m, 1H).

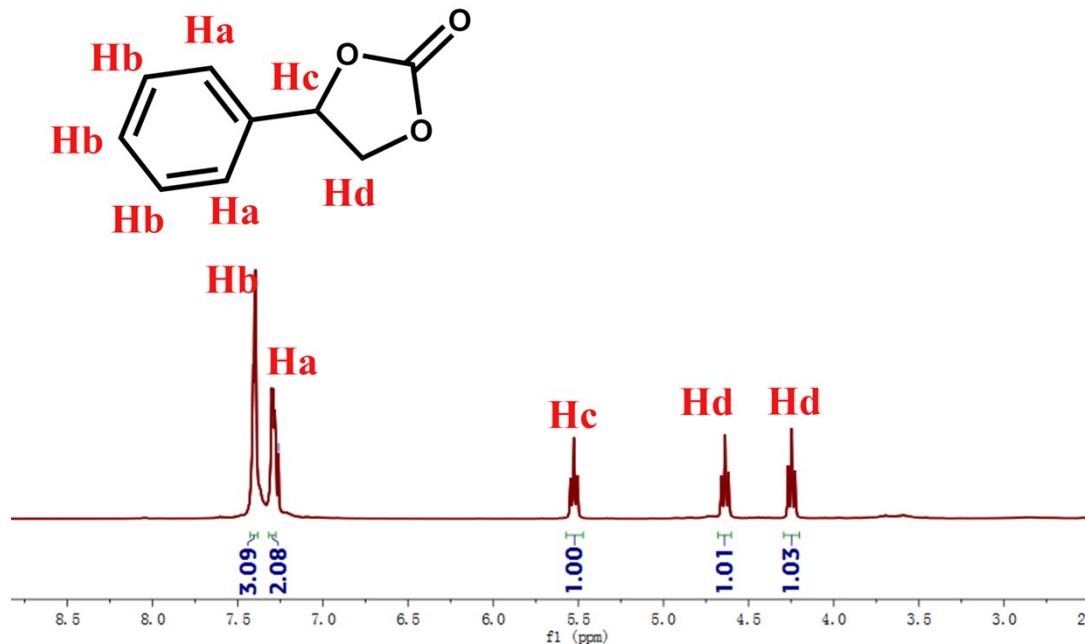


Fig. S22 ^1H NMR of the catalytic product through cycloaddition of CO_2 and 1-phenylcyclopropane (CDCl_3). $\delta = 4.23\text{--}4.27$ (t, 1H), 4.62-4.66 (t, 1H), 5.51-5.55 (t, 1H), 7.28-7.30 (m, 2H), 7.40-7.41 (m, 3H).

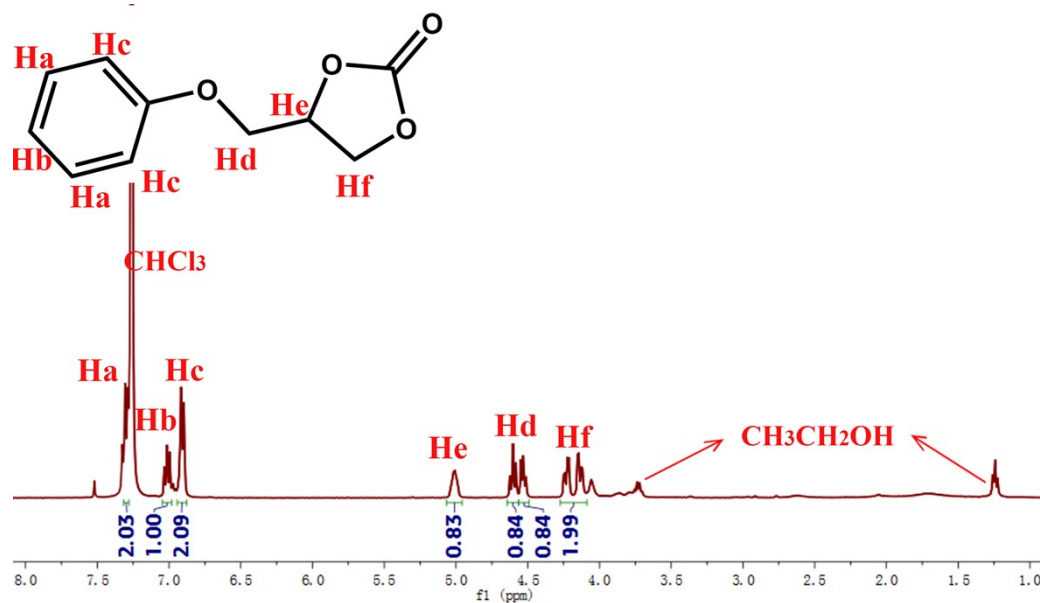


Fig. S23 ^1H NMR of the catalytic product through cycloaddition of CO_2 and 1,2-epoxy-3-phenoxypropane (CDCl_3). $\delta = 4.12\text{-}4.15$ (d, 1H), $4.21\text{-}4.25$ (d, 1H), $4.51\text{-}4.55$ (d, 1H), $4.58\text{-}4.62$ (d, 1H), 5.02 (m, 1H), $6.90\text{-}6.92$ (t, 2H), $7.01\text{-}7.03$ (t, 1H), $7.29\text{-}7.33$ (t, 2H).

Table S2. ICP and EA data of ImBDC-Co and ImBDC-Ni.

Compound		M	C	N	H
ImBDC-Co	ICP	10.54 %			
	Found		40.98 %	6.11 %	5.17%
	Calcd.	10.01%	40.61%	5.03%	5.88%
ImBDC-Ni	ICP	11.20 %			
	Found		41.75%	6.01%	5.32%
	Calcd.	10.24%	41.00%	5.10%	5.58%

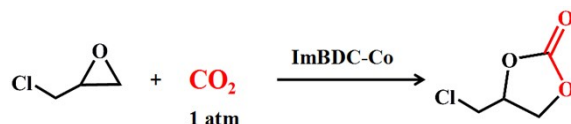
Table S3. XPS data of ImBDC-Co and ImBDC-Ni.

Compound	Element	at%	wt%
ImBDC-Co	I	0.12	0.96
	Cl	0.98	2.20
	S	3.90	7.89
ImBDC-Ni	I	0.17	1.37
	Cl	0	0.00
	S	4.42	8.98

Table S4. The number of noncoordinated anions and solvent molecules in ImBDC-Co and ImBPDC-Ni.

Number	I ⁻	Cl ⁻	SO ₄ ²⁻	DMA	H ₂ O
ImBDC-Co	1	11		27	110
ImBDC-Ni	2		5	21	105

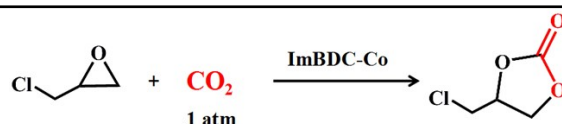
Table S5. The effect of temperature and time on the cycloaddition of CO₂ with epichlorohydrin catalyzed by ImBDC-Co^a.



Entry	T [°C]	Time [h]	Conv. [%]	Yield [%] ^b	Sel. [%]
1	100	24	100	97	97
2	100	12	98	95	97
3	100	6	95	93	98
4	80	12	87	85	89

^aReaction conditions: epoxide (3.0 mmol), ImBDC-Co (29 mg), CO₂ (constant 1 atm), solvent-free. ^bDetermined by GC.

Table S6. The results of cycloaddition of CO₂ and epoxy chloropropane (ECH) catalyzed by three batches of ImBDC-Co^a.




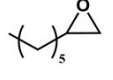
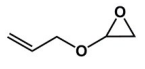
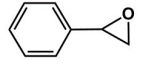
Entry	Catalyst	Conv. [%]	Yield [%] ^b	Sel. [%]
1	ImBDC-Co	96	94	98
2	ImBDC-Co	95	93	98
3	ImBDC-Co	95	92	97

^aReaction conditions: epoxide (3.0 mmol), ImBDC-Co (29 mg), CO₂ (constant 1 atm), solvent-free, temperature (100 °C), time (6 h). ^bDetermined by GC.

Table S7. Comparison of the catalytic activity of the cycloaddition of CO₂ with epichlorohydrin of ImBDC-Co catalyst with previously reported porous materials with functionalized ionic linker.

Catalyst	T [°C]	Pressure [bar]	t [h]	Yield [%]	Ref.
IL@MIL101-SO ₃ H(4)	90	1	24	98	7
FJI-C10	80	1	12	87	8
(I)Meim-UiO-66	120	1	24	94	9
ZnTCPPc(Br)Etim-UiO-66	140	1	14	87	10
UiO-67-IL	90	1	12	88	11
AMIMBr@H ₂ P-DPh COF	120	10	24	91	12
polyILs@MIL-101	70	1	24	94	13
MIL-IMAc-Br ⁻	60	5	24	88	14
2MeIm@Co-BTC-x	90	30	5	97	15
[TMPyPMn(I)] ⁴⁺ (I ⁻) ₄ @ZIF-8	100	1	36	100	16
[Zn(II)NMeTPyP] ⁴⁺ (I ⁻) ₄ @PC N-224	90	8	24	99	17
ImBDC-Co	100	1	6	93	This work

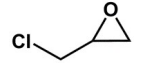
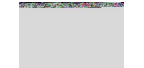


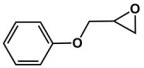
Table S8. Results of cycloaddition of CO₂ and epoxides catalyzed by ImBDC-Co^a

Entry	Substrate	Conv. [%]	Yield [%] ^b	Sel. [%]
1		>99	98	98
2		>99	97	97
3		>99	98	98
4		94	88	94

5		82	80	97
---	---	----	----	----

^a Reaction conditions: epoxide (3.0 mmol), ImBDC-Co (29 mg), CO₂ (constant 1 atm), temperature (120 °C), time (24 h), solvent-free. ^b Determined by GC.

Table S9. Results of cycloaddition of CO₂ and epoxides catalyzed by ImBDC-Ni^a.

Entry	Substrate	Conv. [%]	Yield [%] ^b	Sel. [%]
1		76	73	96
2 ^c		>99	97	97
3 ^c		99	93	94
4 ^c		76	74	97
5 ^c		87	85	96

^aReaction conditions: epoxide (3.0 mmol), ImBDC-Ni (29 mg), CO₂ (constant 1 atm), solvent-free, temperature (100 °C), time (6 h). ^bDetermined by GC. ^c temperature (120 °C), time (24 h).

REFERENCES

- (1) K. H. Cui, S. Y. Yao, H. Q. Li, Y. T. Li, H. P. Zhao, C. J. Jiang and Y. Q. Tian, *CrystEngComm* **2011**, *13*, 3432.
- (2) N. Iki, C. Kabuto, T. Fukushima, H. Kumagai, HaruhikoTakeya, S. Miyanari, T. Miyashi and S. Miyano, *Tetrahedron* **2000**, *56*, 1437-1443.
- (3) N. Iki, H. Kumagai, N. Morohashi, K. Ejima, M. Hasegawa, S. Miyanari and S. Miyano, *Tetrahedron Letters* **1998**, *39*, 7559-7562.
- (4) J. Liang, Y. Q. Xie, X. S. Wang, Q. Wang, T. T. Liu, Y. B. Huang and R. Cao, *Chem. Commun.*, **2018**, *54*, 342-345.5.
- (5) G. M. Sheldrick, *Acta Crystallogr A* **2008**, *64*, 112-122.
- (6) F. R. Dai, U. Sambasivam, A. J. Hammerstrom and Z. Wang, *J. Am. Chem. Soc.* **2014**, *136*, 7480-7491.
- (7) Y. Sun, H. Huang, H. Vardhan, B. Aguila, C. Zhong, J. A. Perman, A. M. Al-Enizi, A. Nafady, S. Ma, *ACS Appl. Mater. Inter.* **2018**, *10*, 27124-27130.
- (8) J. Liang, Y. Q. Xie, X. S. Wang, Q. Wang, T. T. Liu, Y. B. Huang, R. Cao, *Chem. Commun.* **2018**, *54*, 342-345.
- (9) J. Brünig, Z. Csendes, S. Weber, N. Gorgas, R. W. Bittner, A. Limbeck, K. Bica, H. Hoffmann, K. Kirchner, *ACS Catal.* **2018**, *8*, 1048-1051.
- (10) X. Chen, K. Geng, R. Liu, K. T. Tan, Y. Gong, Z. Li, S. Tao, Q. Jiang, D. Jiang, *Angew. Chem. Int. Ed.* **2020**, *59*, 5050-5091.
- (11) N. Huang, P. Wang, M. A. Addicoat, T. Heine, D. Jiang, *Angew. Chem. Int. Ed.* **2017**, *56*, 4982-4986.
- (12) L. G. Ding, B. J. Yao, W. L. Jiang, J. T. Li, Q. J. Fu, Y. A. Li, Z. H. Liu, J. P. Ma, Y. B. Dong, *Inorg. Chem.* **2017**, *56*, 2337-2344.

- (13) Y. Zhang, H. Hu, J. Ju, Q. Yan, V. Arumugam, X. Jing, H. Cai, Y. Gao, *Chin. J. Catal.* **2020**, *41*, 485-493.
- (14) M. Ding, H.-L. Jiang, *ACS Catal.* **2018**, *8*, 3194-3201.
- (15) D. Ma, Y. Zhang, S. Jiao, J. Li, K. Liu, Z. Shi, *Chem. Commun.* **2019**, *55*, 14347-14350.
- (16) Y. Wu, X. Song, S. Xu, J. Zhang, Y. Zhu, L. Gao, G. Xiao, *Catal. Lett.* **2019**, *149*, 2575-2585.
- (17) H. He, Q. Q. Zhu, C. Zhang, Y. Yan, J. Yuan, J. Chen, C. P. Li, M. Du, *Chem. Asian J.* **2019**, *14*, 958-962.